[논문] 수소에너지
J. of the Korean Hydrogen Energy Society
Vol. 9. No. 4(1998)

기계적 합금처리와 수소화물 형성·분해 싸이클링이 Mg의 수소 저장성질에 미치는 영향

송 명 엽

전북대학교, 신소재공학부, 공업기술연구소
전주시 덕진구 덕진동 1가 664-14

Influence of Mechanical Alloying and Hydriding-Dehydriding Cycling on the Hydrogen-Storage Properties of Mg

MyoungYoup Song

Division of New-Materials Engineering, Research Institute of Industrial Technology, Chonbuk National University, 664-14 1ga Deogjindong Deogjingu Chonju Chonbuk, 561-756, Korea

초 록

기계적으로 합금처리한 혼합물 속에 포함된 Mg의 수소 저장 성질의, 시료 내의 Ni의 중량 백분율에 따른 변화를 조사하였다. Ni 중량을 기준으로 한, Mg2Ni 상을 형성한 Ni의 중량 백분율은 Mg-10wt.%Ni 시료에서 가장 높다. 첫번째 수소화물 형성 싸이클에서, Mg의 수소화물 형성 속도에 미치는 기계적 합금처리의 효과는 Mg-25wt.%Ni 시료에서 가장 높다. 활성화 후에는, 기계적 합금처리와 수소화물 형성·분해 싸이클링이 Mg의 수소화물 형성 속도에 미치는 효과는 Mg-10wt.%Ni 시료에서 가장 높다. 충분한 수소화물 형성·분해 싸이클링 후에는, Mg의 수소 저장 용량에 미치는 효과는 Mg-10wt.%Ni에서 가장 높다. Mg의 수소화물 형성 속도와 분해 속도에 미치는 효과는 Mg-25wt.%Ni 시료에서 가장 높다. 시료 내에 포함된 Mg의 수소 저장 성질에 가장 좋은 효과를 가지고 있는 최적의 조성은 Mg-25wt.%Ni이고 그 다음이 Mg-10wt.%Ni이다. 기계적 합금 처리와 수소화물 형성·분해 싸이클링은, 활발한 핵 생성 자리 역할을 할 수 있는 많은 결함을 만들고, 비 표면적을 증가시켜 수소의 확산 거리를 짧게한다.

송명엽

Abstract

The variation of the hydrogen-storage properties of Mg contained in the mechanically-allyed mixture with the weight percentage of nickel in the sample is investigated. The weight percentage of nickel transformed into the Mg2Ni phase, on the basis of the nickel weight, is highest in the Mg-10 wt.%Ni sample. For the first hydriding cycle, the effect of mechanical alloying on the hydriding rate of Mg is highest in the Mg-25 wt.%Ni sample. After activation, the effects of mechanical alloying and hydriding-dehydriding cycling on the hydriding rate of Mg are highest in the Mg-10 wt.%Ni sample. After sufficient hydriding-dehydriding cycling, the effects on the hydrogen-storage capacity of Mg are highest in the Mg-10 wt.%Ni sample. The effects on the hydriding and dehydriding rates of Mg are highest in the Mg-25 wt.%Ni sample. Mg-25wt.%Ni, followed by Mg-10 wt.%Ni, is the optimum composition which has the best effects on the hydrogen-storage properties of Mg contained in the sample. The mechanical alloying and the hydriding-dehydriding cycling produce many defects, which can act as active nucleation sites, and increase the specific surface area, shortening the diffusion distance of hydrogen.

1. Introduction

Magnesium has large hydrogen storage capacity(8.3 wt.%), but its hydriding and dehydriding rates are very low[1] .

In order to improve the reaction kinetics of magnesium with hydrogen, certain metals were alloyed with magnesium[2-7], metal additives were mixed with magnesium8), metal was plated on the surface of magnesium[9] and magnesium hydride was synthesized in the presence of a homogeneous catalyst[10]. In particular for the Mg-Ni-H2 system many researchers have studied the alloying effects[3, 11-14]while Eisenberg et al. have investigated the plating method[9].

In this work, magnesium is alloyed mechanically with nickel to increase the hydriding and dehydriding rates of magnesium. The influence of mechanical alloying and hydriding-dehydriding cycling on the hydrogen-storage properties of Mg contained in the mixtures is investigated.

2. Experimental

For this study magnesium(Alpha) and nickel obtained from nickel carbonyl(3-5 μm) particles were used. Magnesium and nickel mixtures(about 5 g), with compositions Mg-x wt.%Ni(x=5, 10, 25 and 55), were mechanically alloyed under an argon atmosphere in a planetary mill with an acceleration of about 60 ms^{-2} for 5 min. The composition Mg-55 wt.%Ni corresponds to that of Mg2Ni. The planetary mill contained 200 g of stainless

steel balls whose diameters were about 4 mm. Magnesium alone was also treated under the same conditions.

A Sievert's type hydriding-dehydriding apparatus was used for the measurements of hydriding and dehydriding rates. The specific surface areas of the mixture before and after hydriding-dehydriding cycling measured by the BET method by using liquid nitrogen at 77 K. The microstructures of samples before and after hydriding-dehydriding cycling were observed by scanning electron microscope(SEM).

3. Results and Discussions

X-ray diffraction pattern of the samples prepared by the above method showed only magnesium and nickel. With the hydriding-dehydriding cycling, the Mg_2Ni phase formed15). The Mg_2Ni phase is known to have higher hydriding and dehydriding rates than Mg under the same experimental conditions.

Fig.1 shows the variation of the weight percentages of the nickel which is transformed into the Mg_2Ni phase [wt.%Ni(→ Mg_2Ni)] with the weight percentage of nickel (wt.%Ni) at the 10th hydriding cycle at 583 K. The quantities of the wt.%Ni(→ Mg_2Ni) were calculated by measuring the quantities of hydrogen desorbed under a hydrogen pressure under which Mg hydride is stable and only Mg_2Ni hydride decomposes. Curve A concerns the variation of wt.%Ni(→ Mg_2Ni) on the basis of the sample weight, and curve B concerns its variation

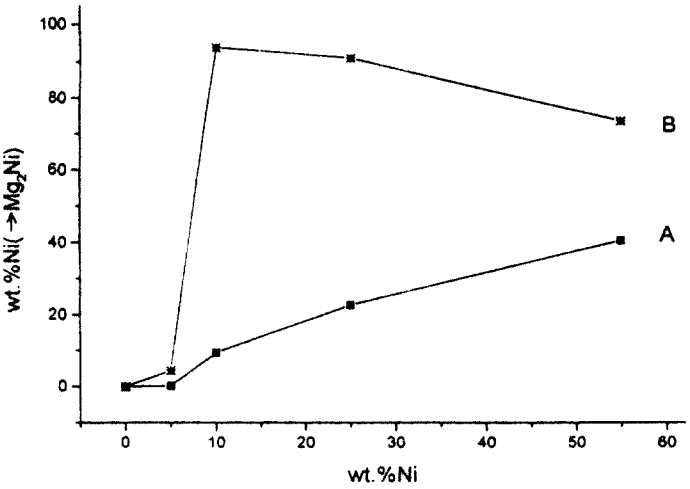

Fig.1 Variation of the weight percentage of nickel transformed into the Mg2Ni phase [wt.% Ni(→ Mg2Ni)] with the weight percentage of nickel(wt.%Ni) on the basis of the sample weight(curve A) and the nickel weight (curve B) at 10th hydriding cycle at 583 K.

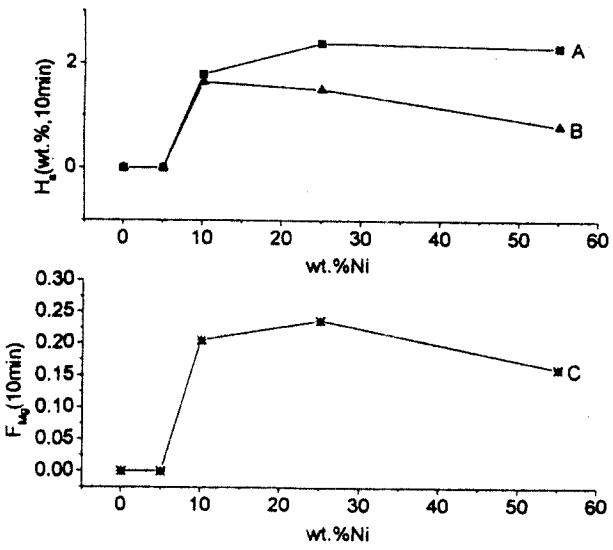

Fig.2 Variation of the weight percentages of hydrogen, for the first hydriding cycle at 573 K 7 barH2,absorbed during 10 min[Ha(wt.%, 10 min)] with wt.%Ni by the sample(curve A) and by Mg(curve B), and variation of the reacted fraction of Mg during 10 min [FMg(10 min)] with wt.%Ni(curve C).

on the basis of the nickel weight contained in the sample. wt.%Ni(→ Mg_2Ni) on the basis of the sample weight increases monotonically with the increase in the wt.%Ni. On the other hand wt.%Ni(→ Mg_2Ni) on the basis of the nickel weight is highest in the Mg-10 wt.%Ni sample, followed in order by the Mg-25 wt.%Ni and Mg-55 wt.%Ni samples. The composition Mg-10wt.%Ni is considered to be the optimum composition for the homogenized mixing of Mg and Ni under our conditions of mechanical alloying.

Fig.2 shows, for the first hydriding cycle at 573 K, 7 bar H_2, the variation of the weight percentages of hydrogen absorbed during 10 min[H_a(wt.%, 10 min)] with the weight percentage of nickel (wt.%Ni). Curve A concerns the variations of H_a(wt.%, 10 min) by the sample, and curve B concerns its variation only by Mg in the sample. H_a(wt.%, 10 min) by Mg was calculated by subtracting the quantity of hydrogen absorbed by the Mg_2Ni phase from H_a(wt.%, 10 min) by the sample. The quantity of the Mg_2Ni phase was obtained by the method explained in Fig.1. The hydriding rate of Mg_2Ni is known much higher than that of Mg. Curve C shows the variation of the reacted fraction of Mg during 10 min[F_{Mg}(10 min)] with wt.%Ni. The samples Mg and Mg-5wt.%Ni does not absorb hydrogen. H_a(wt.%, 10 min) by the sample is highest in the Mg-25 wt.%Ni sample, followed in order by the Mg-55 wt.%Ni and Mg-10 wt.%Ni samples. Ha(wt.%, 10 min) by Mg is highest in the Mg-10 wt.%Ni sample, followed in order by the Mg-25 wt.%Ni and Mg-55 wt.%Ni samples. The reacted fraction of Mg is highest in the Mg-25 wt.%Ni sample, followed in order by the Mg-10 wt.%Ni and Mg-55 wt.%Ni samples. For the first hydriding cycle, the effect of mechanical alloying on the hydriding rate of Mg is highest in the Mg-25 wt.%Ni sample.

In order to compare the hydriding rates of the samples the after activation, we obtained the weight percentages of hydrogen absorbed at 583 K, 8 bar H2 during 10 min[Ha(wt.%, 10 min)] for each sample at the 10th hydriding cycle. Fig. 3 shows its variation with the weight percentage of nickel(wt.%Ni). Curve A concerns the variation of Ha(wt.%, 10 min) by the sample. Curve B concerns its variation only by Mg in the sample. Curve C shows the variation of the reacted fraction of Mg during 10 min[F_{Mg}(10 min)] with wt.%Ni. H_a(wt.%, 10 min) by the sample is highest in the Mg-10 wt.%Ni, followed in order by the Mg-25 wt.%Ni and Mg-55 wt.%Ni samples. H_a(wt.%, 10 min) by Mg and FMg(10 min), respectively, highest in the Mg-10 wt.%Ni sample, followed in order by the Mg-25 wt.%Ni and Mg-5 wt.%Ni. After activation, the effects of mechanical alloying and hydriding-dehydriding cycling on the hydriding rate of Mg are highest in the Mg-10 wt.%Ni sample.

For the comparison of the hydrogen-storage capacities of the samples, we obtained the weight percentages of hydrogen absorbed at 583 K, 8 bar H2

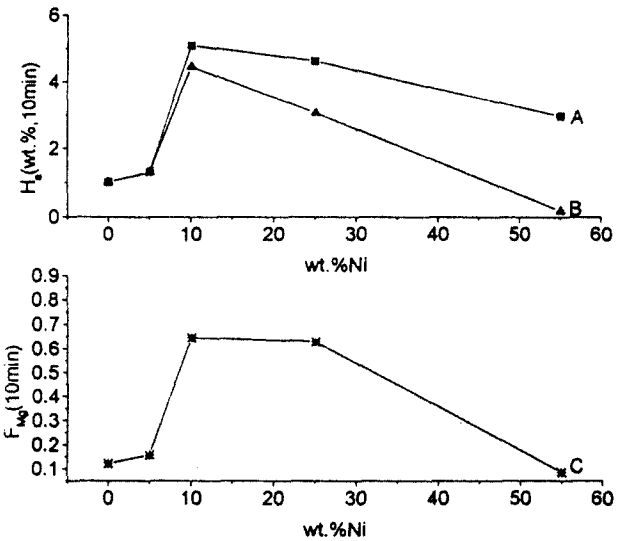

Fig. 3 Variation of the weight percentages of hydrogen absorbed at 583 K, 8 bar H2 during 10 min[Ha(wt.%, 10 min)] at the 10th hydriding cycle with wt.%Ni by the sample(curve A) and by Mg(curve B), and variation of the reacted fraction of Mg during 10 min [FMg(10 min)] with wt.%Ni(curve C).

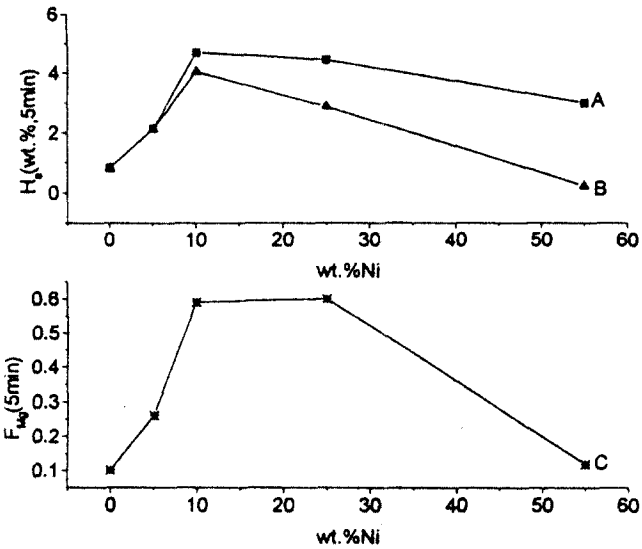

Fig.5 Variation of the weight percentages of hydrogen absorbed at 583 K 8 bar H2 During 5 min[Ha(wt.%, 5 min)] after sufficient hydriding-dehydriding cycling with wt.%Ni by the sample(curve A) and by Mg(curve B), and variation of the reacted fraction of Mg during 5 min [FMg(5 min)] with wt.%Ni (curve C).

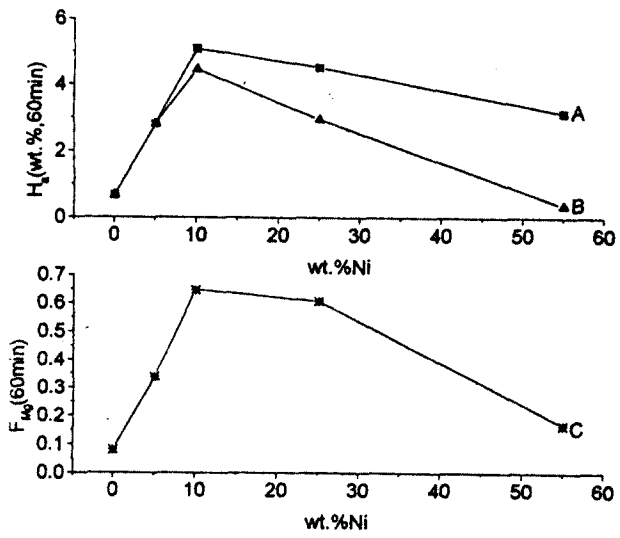

Fig. 4 Variation of the weight percentages of hydrogen absorbed at 583 K 8 bar H2 during 60 min[Ha(wt.%, 60 min)] after sufficient hydriding-dehydriding cycling with wt.%Ni by the sample(curve A) and by Mg(curve B), and variation of the reacted fraction of Mg during 60 min [FMg(60 min)] with wt.%Ni(curve C).

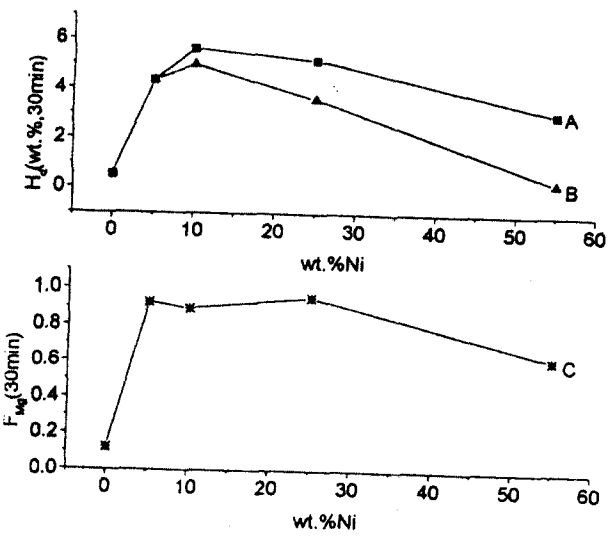

Fig.6 Variation of the weight percentages of hydrogen desorbed at 583 K 1.5 bar H2 during 30 min [Hd(wt.%, 30 min)] after sufficient hydriding-dehydriding cycling with wt.%Ni by the sample(curve A) and by Mg(curve B) , and variation of the reacted fraction of Mg during 30 min [FMg(30 min)] with wt.%Ni(curve C).

during 60 min[H_a(wt.%, 60 min)] for each sample after the samples were sufficiently hydriding-dehydriding cycled. Fig. 4 shows its variation with the weight percentage of nickel(wt.%Ni). Curve A concerns the variation of Ha(wt.%, 60 min) by the sample. Curve B concerns its variation only by Mg in the sample. Curve C shows the variation of the reacted fraction of Mg during 60 min [FMg(60 min)] with wt.%Ni. Ha(wt.%, 60 min) by the sample is highest in the Mg-10 wt.%Ni sample, followed in order by the Mg-25 wt.%Ni and Mg-55 wt.%Ni samples. H_a(wt.%, 60 min) by Mg is highest in the Mg-10 wt.%Ni sample, followed in order by the Mg-25 wt.%Ni and Mg-5 wt.%Ni samples. FMg(60 min) is highest in the Mg-10 wt.%Ni sample, followed in order by the Mg-25 wt.%Ni and Mg-5 wt.%Ni samples. After the samples are sufficiently hydriding-dehydriding cycled, the effects of mechanical alloying and hydriding-dehydriding cycling on the hydrogen-storage capacity of Mg are highest in the Mg-10 wt.%Ni sample.

In order to compare the hydriding rates of the samples after sufficient hydriding-dehydriding cycling, we obtained the weight percentages of hydrogen absorbed at 583 K, 8 bar H_2 during 5min[H_a(wt.%, 5 min)] for each sample. Fig.5 shows its variation with the weight percentage of nickel(wt.%Ni). Curve A concerns the variation of H_a(wt.%, 5 min) by the sample. Curve B concerns its variation only by Mg in the sample. Curve C shows the variation of the reacted fraction of Mg during 5 min[F_{Mg}(5 min)] with wt.%Ni. H_a(wt.%, 5 min) by the sample is highest in the Mg-10 wt.%Ni, followed in order by the Mg-25 wt.%Ni and Mg-55 wt.%Ni samples. Ha(wt.%, 5 min) by Mg is highest in the Mg-10 wt.%Ni sample, followed in order by the Mg-25 wt.%Ni and Mg-5 wt.%Ni samples. F_{Mg}(5 min) is highest in the Mg-25 wt.%Ni sample, a little higher than that of the Mg-10 wt.%Ni sample, then followed by the Mg-5 wt.%Ni sample. After sufficient hydriding-dehydriding cycling, the effects of mechanical alloying and hydriding-dehydriding cycling on the hydriding rate of Mg are highest in the Mg-25 wt.%Ni sample.

For the comparison of dehydriding rates of the samples after sufficient hydriding-dehydriding cycling, we obtained the weight percentages of hydrogen desorbed at 583 K, 1.5 bar H2 during 30 min [H_d(wt.%, 30 min)] for each sample. Fig.6 shows its variation with wt.%Ni. Curve A concerns the variation of H_d(wt.%, 30 min) by the sample. Curve B concerns its variation only by Mg in the sample. Curve C shows the variation of the reacted fraction of Mg during 30 min [F_{Mg}(30 min)] with wt.%Ni. H_d(wt.%, 30 min) by the sample is highest in the Mg-10 wt.%Ni sample, followed in order by the Mg-25 wt.%Ni and Mg-5 wt.%Ni samples. H_d(wt.%, 30 min) by Mg is highest in the Mg-10 wt.%Ni sample, followed in order by the Mg-5 wt.%Ni and Mg-25 wt.%Ni samples. F_{Mg}(30 min) is highest in the

Table. 1. The effects of mechanical alloying and hydriding-dehydriding cycling on the hydrogen-storage properties of Mg(The smaller number means the better hydrogen storage property).

Samples property	Mg	Mg-5wt.%Ni	Mg-10wt.%Ni	Mg-25wt.%Ni	Mg-55wt.%Ni
transformation into Mg_2Ni phase	-	4	1	2	3
hydriding rate at n=1	4	4	2	1	3
hydriding rate after activation	4	3	1	2	5
hyrogen-storage capacity	5	3	1	2	4
hydriding rate after sufficient cycling	5	3	2	1	4
dehydriding rate after sufficient cycling	5	2	3	1	4
total	23	15	9	7	20
rating	5	3	2	1	4

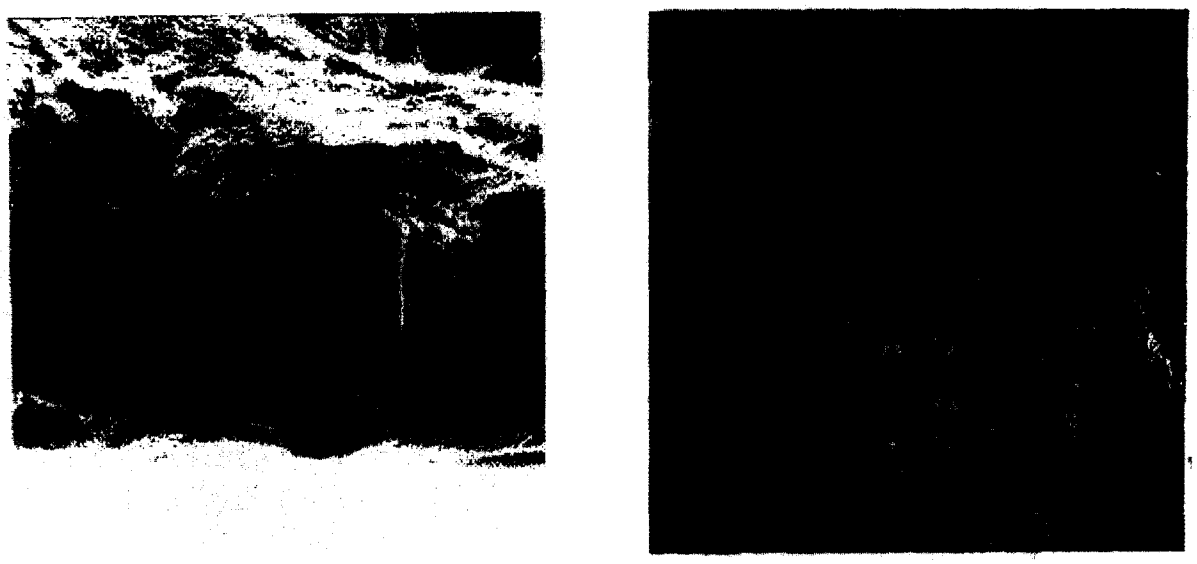

(a) (b)

Fig.7 Microstructures, observed by SEM, for (a)the cleavage surface of the mechanically-treated Mg before hydriding-dehydriding cycling(×650) and (b)the Mg-5wt.%Ni sample after 6 hydriding-dehydriding cycles(×700).

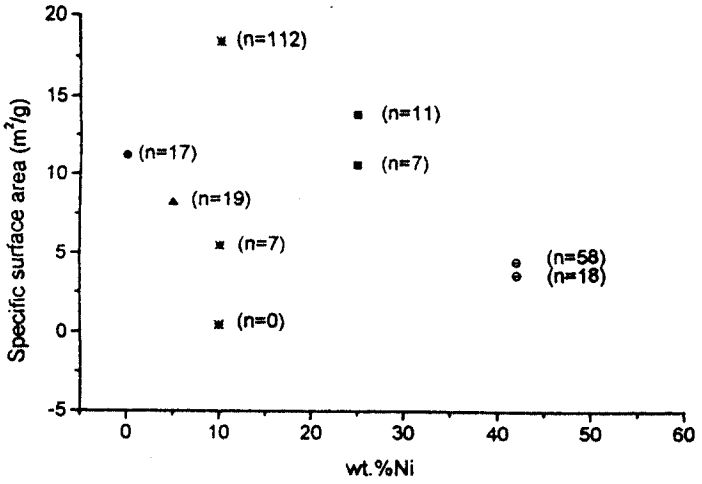

Fig.8 Variation of the specific surface area(m^2 /g) with wt.%Ni at various hydriding-dehydriding cycles(n).

Mg-25 wt.%Ni, followed in order by the Mg-5 wt.%Ni and Mg-10 wt.%Ni samples. After sufficient hydriding-dehydriding cycling, the effects of mechanical alloying and hydriding-dehydriding cycling on the dehydriding rate of Mg are highest in the Mg-25 wt.%Ni sample.

The Mg-10 wt.%Ni sample shows the best performance in the hydriding rate of Mg after activation, and the hydrogen-storage capacity of Mg. The Mg-25 wt.%Ni sample shows the best performance in the hydriding rate of Mg for the first cycle, and the hydriding and dehydriding rate of Mg after sufficient hydriding-dehydriding cycling.

The effects of mechanical alloying and hydriding-dehydriding cycling on the hydrogen-storage properties of Mg are summarized in Table 1. The numbers are the orders of the mechanically-alloyed mixtures for each hydrogen storge property of Mg. The smaller number means the better hydrogen storage property. Mg-25 wt.%Ni, followed by Mg-10 wt.%Ni, is the optimum composition which has the best effects on the hydrogen-storage properties of Mg contained in the sample.

Fig.7 shows the microstructures, observed by SEM, for cleavage surface of the mechanically-treated Mg before hydriding-dehydriding cycling [Fig. 7(a)] and of the Mg-5 wt.%Ni sample after 6 hydriding-dehydriding cycles[Fig. 7(b)]. The cleavage surface of the mechanically-treated Mg is relatively smooth. The Mg-5 wt.%Ni sample shows a surface which is very irregular and has many defects, with the surface area increased. The defects are considered to act active nucleation sites for the hydrides and the α-solid solutions of Mg_2Ni and/or Mg.

Fig.8 shows the variation of the specific surface area (m^2/g) with the weight percentage of nickel (wt.%Ni) at various hydriding-dehydriding cycles(n). For the same sample, the specific surface area increases with the increase in the number of hydriding-dehydriding cycles(n). From the points for the Mg-10 wt.%Ni, we can see that during earlier cycles the specific surface area increases rapidly with cycling and it increases slowly during later cycles. The specific surface area of Mg-55wt.%Ni increases very slowly from n=18 to n=58. The enlargement in the

specific surface area decrease the particle size, shortening the diffusion distance of hydrogen in the hydriding and dehydriding reactions. The points for similar cycles(n=7-19) shows that the specific surface area decreases with the increase in the wt.%Ni.

4. Conclusions

The weight percentage of nickel transformed into the Mg_2Ni phase, on the basis of the nickel weight, is highest in the Mg-10 wt.%Ni sample.

For the first hydriding cycle, the effect of mechanical alloying on the hydriding rate of Mg are highest in the Mg-25 wt.%Ni sample. After activation, the effects of mechanical alloying and hydriding-dehydriding cycling on the hydriding rate of Mg are highest in the Mg-10 wt.%Ni sample.

After sufficient hydriding-dehydriding cycling, the effects on the hydrogen-storage capacity of Mg is highest in the Mg-10 wt.%Ni sample. The effects on the hydriding and dehydriding rates of Mg are highest in the Mg-25 wt.%Ni sample.

Mg-25 wt.%Ni, followed by Mg-10 wt.%Ni, is the optimum composition which has the best effects on the hydrogen-storage properties of Mg contained in the sample.

The mechanical alloying and the hydriding-dehydriding cycling produce many defects, which can act as active nucleation sites, and increase the specific surface area, shortening the diffusion distance of hydrogen.

Acknowledgement

The financial support of the Korean Science & Engineering Foundation(KOSEF, Serial No. 901-0610-011-2) is gratefully acknowledged.

References

1. A. Vose, Metal Hydrides, U.S. Patent 2 944, p. 587(1961).
2. J. J. Reilly and R. H. WisWall, Inorg. Chem. 6. (1967)2220.
3. J. J. Reilly and R. H. WisWall, Jr, Inorg. Chem. 7, (1968)2254.
4. D. L. Douglass, Metall. Trans. A, 6, (1975)2179.
5. M. H. Mintz, Z. Gavra and Z. Hadari, J. Inorg, Nucl. Chem. 40, (1978)765.
6. M. Pezat, A. Hbika, B. Darriet and P. Hagenmuller, French Anvar Patent 78 203 82, 1978. Mater, Res. Bull. 14, (1979)377.
7. M. Pezat, B. Darriet and P. Hagenmuller, J. Less-Common Met., 74 (1980) 427.
8. B. Tanguy, J. L. Soubeyroux, M. Pezat, J. Portier and P. Hagenmuller, Mater. Res. Bull. 11, (1976)1441.
9. F. G. Eisenberg, D. A. Zagnoli and J. J. Sheridan Ⅲ, J. Less-Common Met., 74, (1980)323.

10. B. Bogdanovic, Int. J. Hydrogen Energy, 9, (1984)937.

11. E. Akiba, K. Nomura, S. Ono and S. Suda, Int. J. Hydrogen Energy, 7, (1982) 787.

12. E. Akiba, K. Nomura, S. Ono, J. Less-Common Met., 89, (1983)145.

13. J. M. Boulet and N. Gerard, J. Less-Common Met., 89, (1983)151.

14. S. Ono, Y. Ishido, E. Akiba, K. Jindo, Y. Sawada, I. Kitagawa and T. Kakutani, in T. N. Veziroglu and J. B. Taylor(eds), Hydrogen Energy Progress V, Proc. 5th World Hyrogen Energy Conf., Toronto, Canada, Vol. 3, pp. 1291-1302. Pergamon, New York(1984).

15. M. Y. Song, J. of the Korean Hydrogen Energy Society, 9(2) (1998)47.